Explaining hysteresis in electronic circuits

A. S. Elwakil
Department of Electrical and Electronic Engineering, University of Sharjah, Sharjah, United Arab Emirates
E-mail: elwakil@ee.ucd.ie, elwakil@sharjah.ac.ae

Abstract We show how the hysteresis behaviour in electronic circuits can be explained in a robust manner using PSpice transient simulations. Furthermore, we describe a simple circuit for three-segment nonlinear characteristic shaping and show how this circuit can be used to produce hysteresis loops. The realisation of relaxation oscillators is then given as a typical application.

Keywords amplifiers; hysteresis; nonlinear circuits; nonlinear dynamics

Undergraduate electronic circuits textbooks, such as Ref. 1, introduce the hysteresis phenomena to their readers while attempting to explain the behaviour of a simple op-amp comparator with positive feedback. Such a circuit is then characterized as *bi-stable*; i.e. it has two different driving point characteristics depending on whether the input voltage is increasing or decreasing. When plotted together on the same V_i-V_o chart, a discontinuous loop appears and is termed the hysteresis loop. The sudden *jumps* in the loop are attributed to the bi-stable nature of the circuit and are not discussed any further.

From a nonlinear dynamics point of view, sudden jumps correspond to very fast energy transfer. Accordingly, an energy storage element (capacitor or inductor) of a significantly small value must exist to hold this transit energy transfer. Including a parasitic capacitor (inductor) is necessary but not sufficient to explain the hysteresis jumps, as explained in detail in the pioneering work of Kennedy and Chua[2] which ironically never found its way to any textbook. In particular, the two necessary conditions for hysteresis to occur are:

1 A static d.c. nonlinear non-monotone driving-point characteristic.
2 A parasitic energy storage element to accommodate the fast energy transfer. This fast transition is described by a stiff differential equation (one which contains two widely separated time constants).

The work presented here has two objectives:

(i) To show how the hysteresis behaviour can be explained in a clear manner with a circuit simulation example.
(ii) To show how nonlinear driving-point characteristics can be designed.

Explaining hysteresis

To explain hysteresis, one should address the two necessary conditions stated above. The first condition relates to the existence of d.c. nonlinear characteristics. In Fig. 1, the four basic nonlinear characteristics which can be obtained from any

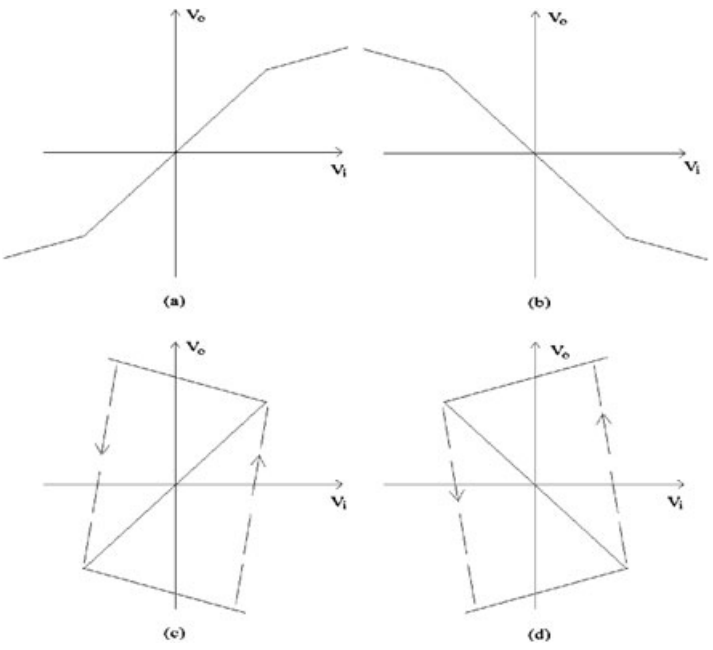

1

Fig. 1 *Four basic three-segment nonlinear characteristics; (a) & (b) monotone nonlinearities, (c) & (d) nonmonotone nonlinearities giving rise to hysteresis.*

three segments are shown. The characteristics of Figs 1(a) and 1(b) are monotone which means they are equally controllable via the *x*-axis or the *y*-axis variable. A single value for *x* corresponds to a single value for *y*. However, Figs 1(c) and 1(d) are non-monotone because they are controllable only through the *y*-axis variable. Attempting to control these characteristics through the *x*-axis variable results in multiple values of *y* for the same value of *x*, which is not possible in electronic circuits. Accordingly, the apparent characteristics acquire 'discontinuous jumps' and follow the dashed lines in Fig. 1. Stimulating hysteresis is thus associated with controlling a nonlinear non-monotone driving-point characteristic via the *wrong* control variable.

In order to explain the 'jump' phenomena, which is a result of a fast energy transfer process, nonlinear dynamics principles[3] imply that a *transit* (parasitic) energy storage element (capacitor or inductor) is necessary to accurately model this behaviour[4]. An inductor (capacitor) is considered for current (voltage)-controlled characteristics. To demonstrate this, the active tank oscillator, shown in the upper-right corner of Fig. 2, is taken as an example. This classical sinusoidal oscillator employs a voltage-controlled negative resistor, which can be implemented using an op-amp, as shown in the lower-left corner of the same figure. However, this negative resistor has a limited linear range (due to the op-amp saturation voltage) and on

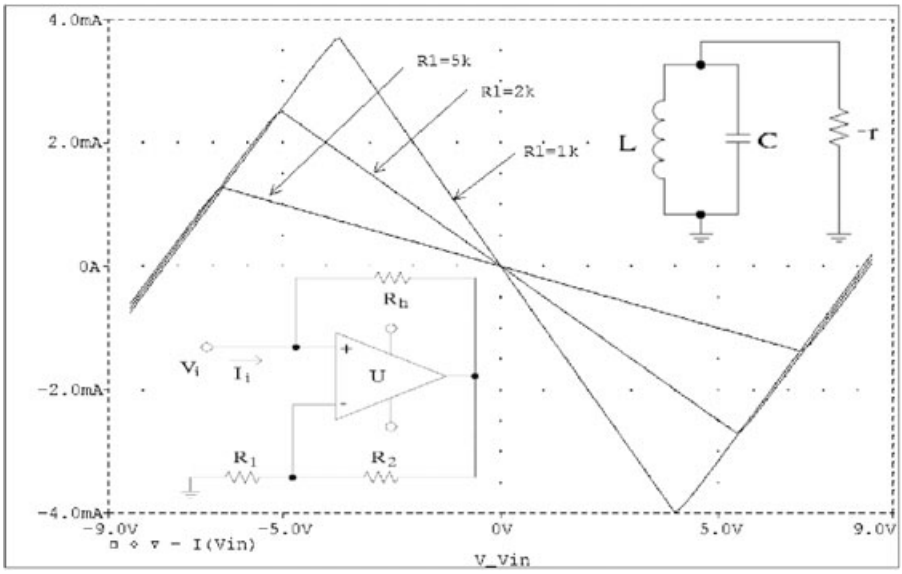

Fig. 2 *Active tank oscillator (upper right) using a voltage-controlled negative resistor (lower left) and PSpice d.c. simulation of its characteristics* ($R_2 = R_h = 1\,k\Omega$, *±9 V supplies).*

the full range it is essentially nonlinear, as indicated by the PSpice d.c. simulation of Fig. 2. It is clear that this nonlinear resistor is non-monotone and should not be controlled by the *y*-axis variable; i.e. the input current. Attempting to use this nonlinear negative resistor in a current-controlled, rather than voltage-controlled, structure will stimulate hysteresis.

In the active tank oscillator of Fig. 2, the capacitor voltage is used properly to control the negative resistor, hence sinusoidal oscillations are produced and hysteresis is avoided as shown in Figs 3(a) and (b) which are obtained from PSpice transient simulations with $L = 10\,\text{mH}$ and $C = 100\,\text{nF}$. Fig. 3(a) represents the sinusoidal output waveform while Fig. 3(b) is the negative resistor nonlinear characteristics dynamically plotted during the transient simulations. The following Figs 3(c)–3(f) demonstrate what happens when the capacitor value is reduced to 1 nF and then to 300 pF respectively. Evidently, hysteresis appears and is clearly visible in Fig. 3(f). The reason is that by reducing the capacitor, while keeping the inductor sufficiently large, we are attempting to use the inductor current, instead of the capacitor voltage, to control the nonlinear resistor, hence stimulating hysteresis. Note from Fig. 3 that the sinusoidal waveform gradually disappears and is replaced with a saw-tooth waveform as the capacitor value decreases. This indicates the existence of slow-fast dynamics resulting from the fast energy transfer during hysteresis. In other words, the sinusoidal oscillator transforms into a relaxation oscillator[5].

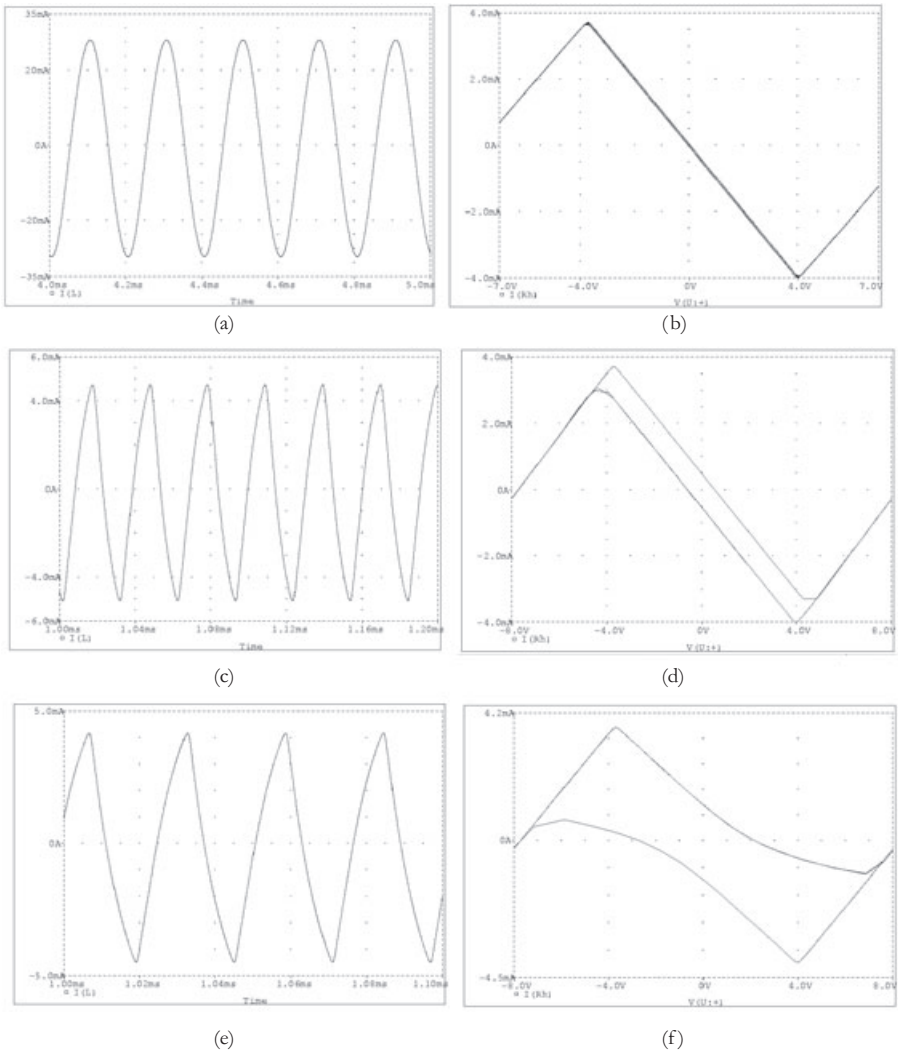

Fig. 3 *PSpice simulations showing the effect of reducing the capacitor value in the active tank oscillator. Simulations performed with* L = *10 mH,* C = *100 nF, 1 nF and 300 pF respectively along with the characteristics of Fig. 2 when* R_1 = *1 k*Ω.

Nonlinear characteristic shaping

The second objective of this work is to show how the monotone and non-monotone three-segment characteritics in Fig. 1 can be designed. It is usually desired to obtain voltage transfer characteristics, i.e. a V_i-V_o nonlinear relation. However, it is also possible to obtain I_i-I_o, V_i-I_o or I_i-V_o nonlinear relations via appropriate *I-V* or *V-I* conversion techniques. Traditional nonlinear shaping circuits, which can be found

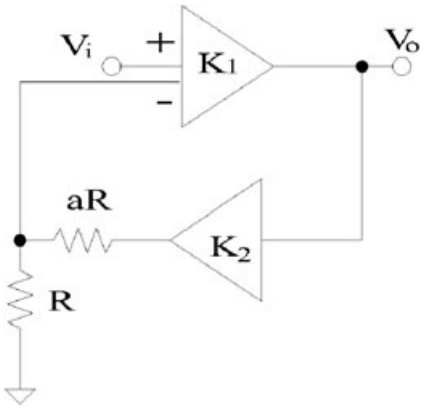

Fig. 4 *Proposed two-amplifier structure for realising 3-segment nonlinear characteristics.*

in undergraduate textbooks or even in research articles,[6–8] employ diodes or diode-connected transistors to create the breakpoints in the nonlinear characteristics. Here, we describe a novel, yet simple, two-amplifier circuit which can be used to realise all four characteristics of Fig. 1 using only the typical amplifier saturation characteristics[1] without diodes or transistors.

The proposed circuit is shown in Fig. 4 employing two amplifiers, one of which is differential, and a potential divider. Assume both amplifiers operate in their linear regions with d.c. gains K_1 and K_2 respectively, it is easy to show that

$$\frac{V_o}{V_i} = \frac{K_1(1+a)}{1+K_1K_2+a} \tag{1}$$

where $a > 1$. If both amplifiers have the same saturation voltage V_{sat}, then it is clear from Fig. 4 that amplifier K_2 will reach saturation before amplifier K_1. In this case, the output of K_2 will remain fixed at V_{sat} whereas K_1 will remain in its linear region. Hence the V_i-V_o relation becomes

$$V_o = K_1\left(V_i - \frac{V_{sat}}{1+a}\right) \tag{2}$$

From (1) and (2) we note that a breakpoint in the characteristics occurs at $V_i = V_{sat}\left(\frac{1}{K_2}+\frac{K_1}{1+a}\right)$. The slope of the linear segment after the breakpoint (outer segment) depends only on K_1 while that of the segment before the breakpoint (inner segment) depends on both K_1 and K_2. The location of the breakpoint depends on K_1, K_2 and a. Therefore, one can independently adjust the slopes of the linear segments and the location of the breakpoint. Note that K_1 and K_2 can be made positive or negative depending on whether the amplifiers are inverting or

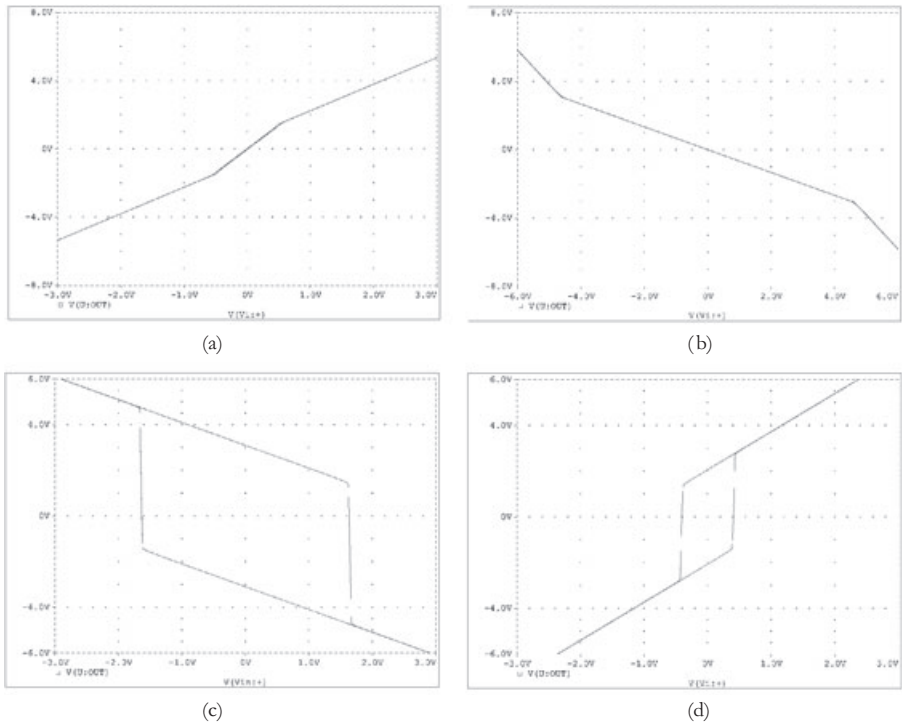

Fig. 5 *PSpice simulations of the obtained nonlinear characteristics of Fig. 4 using op-amp based amplifiers biased with ±7 V supplies; (a)* (K_1,K_2,a) *= (2,–1,3), (b)* (K_1,K_2,a) *= (–4,1,1), (c)* (K_1,K_2,a) *= (–4,1,4), (d)* (K_1,K_2,a) *= (–2,–2,2).*

noninverting. Table 1 summarises the different possibilities and the resulting nonlinear characteristics.

Of course, the two amplifiers can be implemented using any suitable device. However, to verify the proposed functionality, we perform PSpice simulations after implementing K_1 and K_2 using standard op amp-based amplifiers.[1] Figs 5(a)–5(d) show the four obtained nonlinear relations using the parameter sets (K_1, K_2, a) = (2, –1, 3), (–4, 1, 1), (–4, 1, 4), (–2, –2, 2) respectively. Note the appearance of the hysteresis loops in Figs 5(c) and 5(d) resulting from the non-monotonicity of the characteristics.

As a direct application, we choose the settings leading to the hysteresis loop of Fig. 5(d) and then connect a capacitor C in the feedback; i.e. between the V_i and V_o terminals (see Fig. 4) while terminating V_i with a grounded resistor R. As expected, the resulting structure is a realxation oscillator[5] and the observed V_o and V_c PSpice simulation waveforms are plotted in Fig. 6(a) for $R = 10\,\text{k}\Omega$ and $C = 10\,\text{nF}$. The hysteresis loop of Fig. 5(c) can also be used for the same purpose, as shown in Fig. 6(b); however, R and C need to interchange their positions in this case.

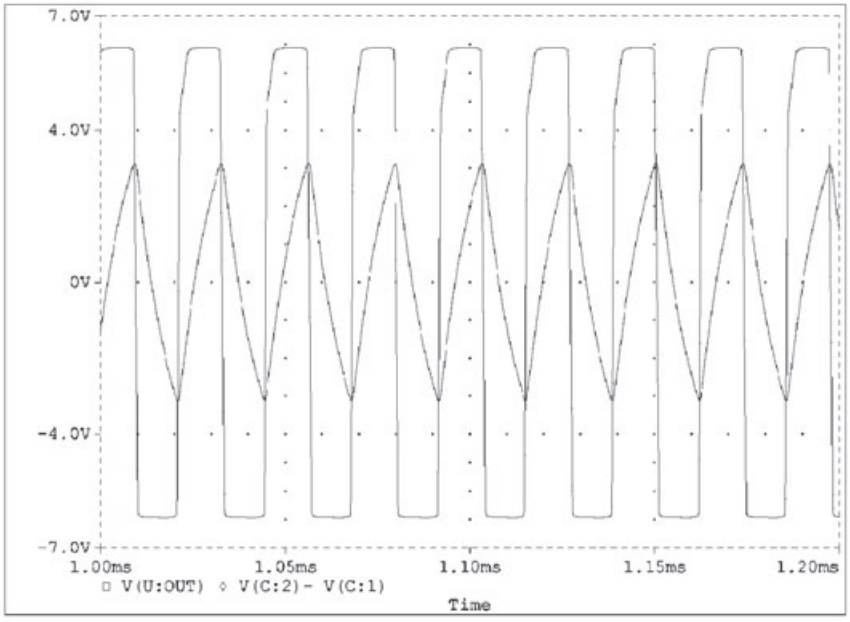

(a)

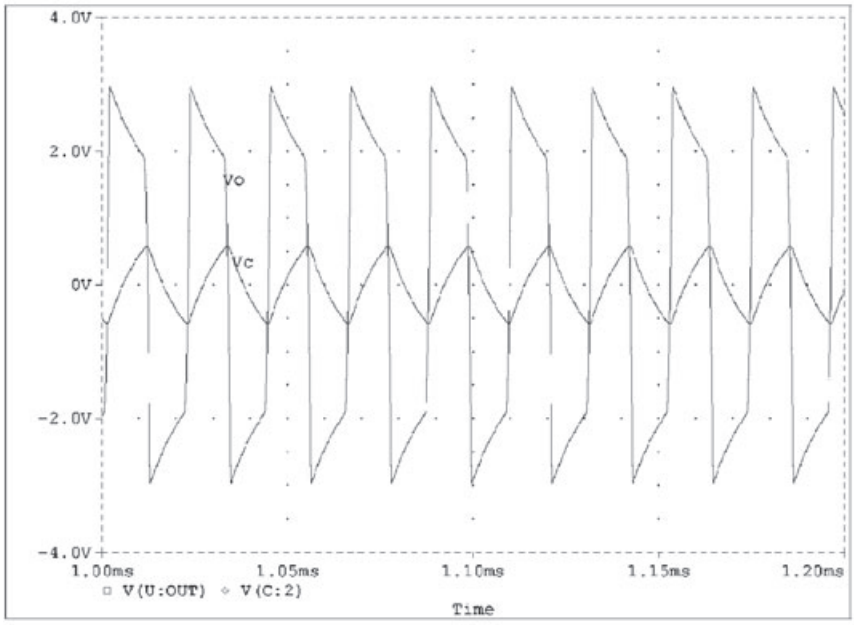

(b)

Fig. 6 *PSpice simulations of the waveforms of two relaxation oscillators obtained using Fig. 4 when realising the hysteresis loops of (a) Fig. 5(d) and (b) Fig. 5(c).*

TABLE 1 *Summary of the different possibilities for* K_1 *and* K_2 *in Fig. 4 and the resulting characteristics*

K_1	K_2	S_{inner}	S_{outer}	Figure
+	+	+	+	1(*a*)
−	+	− if $\lvert K_1K_2\rvert < 1 + a$	−	1(*b*)
		+ if $\lvert K_1K_2\rvert > 1 + a$		1(*c*)
+	−	− if $\lvert K_1K_2\rvert > 1 + a$	+	1(*d*)
		+ if $\lvert K_1K_2\rvert < 1 + a$		1(*a*)
−	−	−	−	1(*b*)

Finally, and to evaluate the frequency response of the structure, we assume single pole models for the two amplifiers; that is $k_1 = K_1\omega_1/(s + \omega_1)$ and $k_2 = K_2\omega_2/(s + \omega_2)$ where $\omega_{1,2}$ are the gain-bandwidth products. In the inner segment of the nonlinearity, it can be shown that

$$\frac{V_o}{V_i} = \left(\frac{K_1(1+a)}{1+K_1K_2+a}\right)\frac{1+\dfrac{1}{\omega_2}s}{1+\dfrac{(1+a)(\omega_1+\omega_2)}{(1+K_1K_2+a)\omega_1\omega_2}s+\dfrac{(1+a)}{(1+K_1K_2+a)\omega_1\omega_2}s^2} \tag{3}$$

which indicates that the phase error can be minimised (by equating the numerator and denominator s coefficients) if $a = K_1K_2\frac{\omega_1}{\omega_2} - 1$. This is possible only if $K_1K_2\frac{\omega_1}{\omega_2} > 1$; i.e. $K_{1,2}$ are both positive or both negative. Therefore, Figs 1(a) and 1(b) are better realised using rows one and four of Table 1.

Conclusion

We have shown how the hysteresis behaviour can be explained in a robust manner, avoiding the so called 'bi-stable' explanation. A simple circuit which can be used to design hysteresis loops was then proposed. This work should prove useful while teaching the nonlinear behaviour of amplifiers limited by their saturation voltage, which is dictated by the supply voltage.

References

1 A. S. Sedra and K. C. Smith, *Microelectronic circuits* (Oxford University Press, New York, 1998).
2 M. P. Kennedy and L. O. Chua, 'Hysteresis in electronic circuits: A circuit theorist's perspective', *Int. J. Circuit Theory Appl.*, **19** (1991), 471–515.
3 L. O. Chua, C. A. Desoer and E. S. Kuh, *Linear and Nonlinear Circuits* (McGraw-Hill, New York, 1987).
4 L. O. Chua and P. M. Lin, *Computer-Aided Analysis of Electronic Circuits* (Prentice-Hall, Englewood Cliffs, 1975).
5 A. S. Elwakil, 'Low voltage relaxation oscillator', *Electron. Lett.*, **36** (2000), 1256–1257.
6 S. Liu, D. Wu, H. Tsao and J. Tsay, 'Nonlinear circuit applications with current conveyors', *IEE Proc. Circuits Devices Syst.*, **140** (1993), 1–6.

7 S. Kutta, 'Current mode circuit implementation of PWL functions', *Analog Integrated Circuits Signal Process.* **16** (1998), 285–297.
8 E. Sanchez-Sinencio, J. Ramirez-Angulo, B. Linares-Barranco and A. Rodriguez-Vazquez, 'Operational transconductance amplifier-based nonlinear function syntheses', *IEEE J. Solid-State Circuits*, **24** (1989), 1576–1586.